Mean-Field Study of Normal Metal-Quantum Dot-Superconductor System in the Presence of External Magnetic Field

Pujita Das,[a] Sachin Verma,[b] and Ajay[c]

Department of Physics, Indian Institute of Technology Roorkee Uttarakhand, India 247667.

[a]Corresponding author: p_das@ph.iitr.ac.in
[b]sverma2@ph.iitr.ac.in
[c]ajay@ph.iitr.ac.in

Abstract. In this paper, we have analyzed the spectral and transport properties of a weakly correlated single-level quantum dot hybridized with one normal conducting and another Bardeen–Cooper–Schrieffer (BCS) superconducting lead (N-QD-S system) in the presence of an external magnetic field. We have employed Green's function equation of motion (EOM) approach within a self-consistent Hartree-Fock (HF) mean-field approximation to analyze the Hamiltonian. We studied the effect of on-dot Coulomb correlation and an external magnetic field on the sub-gap Andreev levels of a quantum dot, strongly coupled to a conventional s-wave superconductor as a function of impurity parameters. We have shown that for a finite magnetic field, the Andreev bound states (ABSs) split into a spin-up and spin-down contribution (i.e. Zeeman splitting) and cross the Fermi energy level, resulting in a quantum phase transition, which is an indication of a change in the fermion parity of the ground state. Further, within the non-linear regime, we discuss the total electrical conductance for various values of Zeeman energy and on-dot Coulomb interactions. We have compared our results with the existing experimental and theoretical results.

INTRODUCTION

Quantum dot (QD) [1] or quantum impurity coupled to a conventional superconductor offers nontrivial phenomena and has been a topic of intensive study for the past few decades due to its potential application in the field of nanoelectronics. The richness of its physical phenomena associated with superconductor-QD hybrid systems has been discovered in a great variety of setups, such as magnetic adatoms [2], self-assembled QDs [3], nanowire QDs [4], carbon nanotube QDs [5], and graphene QDs [6]. It has been widely used in nanoelectronic devices such as superconducting quantum interference devices [7], Cooper pair splitters [8], superconducting quantum computers [9], and topological quantum information processing [4]. In addition to that, the unique properties of such hybrid nanodevices make them promising platforms to study fundamental phenomena such as the quantum interference effect [10] and Majorana fermions [4].

When a normal-type (N) conductor is connected to a superconductor (S), a superconducting order parameter can leak into it, giving rise to pairing correlations and an induced superconducting gap. This phenomenon, known as the superconducting proximity effect, forms new sub-gap states known as Andreev bound states (ABSs). In this case, the superconducting proximity effect competes with the Coulomb blockade effect, which comes from the electrostatic repulsion among the electrons of the quantum dot (QD). At low temperatures, additionally, one crucial effect comes into play known as the Kondo physics. Both these phenomena, i.e., Coulomb blockade and the appearance of a Kondo singlet state, compete with the induced on-dot pairing. In this present study, we exclude the Kondo effect, and only the competition between the Coulomb blockade effect and induced on-dot pairing is analyzed. Besides, when such hybrid structures are exposed to the magnetic field, the proximity effect allows for interplay between superconductivity and magnetism, which gives rise to a variety of interesting effects. In nanoscopic tunneling junctions, a wide range of important physical phenomena can be explored by varying the QD hybridization with the superconducting lead, applying a magnetic field, and controlling the temperature (lowering the temperature can activate the Kondo effect).

Here, we have addressed the subgap ABS transport properties of a single-level quantum dot coupled to normal and BCS superconductor reservoirs (N-QD-S) in the Coulomb blockade regime in the absence and presence of an external magnetic (Zeeman) field. Also, we have analyzed the formation of Andreev-bound states in this particular N-QD-S system [see Figure 1]. We employ the equation-of-motion (EOM) technique within a self-consistent Hartree Fock (HF) mean-field approximation to describe the Coulomb blockade regime. One can use different types of higher-order decoupling schemes in the context of the EOM technique to investigate hybrid systems both in the Coulomb blockade and the Kondo regime [14, 17].

We would like to investigate the case of a Zeeman-split dot energy level. As for the case of non-interacting dot electrons, the energy levels are spin-independent. But, even if we apply a small enough magnetic field B, the dot level splits into two levels, where the higher level is occupied by the spin-up electron and the lower level by the spin-down electron. We show the singlet to doublet transition of ABSs for different U (Coulomb interaction), Δ_{sc} (superconducting gap), Γ_s (coupling to the superconducting lead) values irrespective of B-field (external magnetic field). Most importantly, the B-field dependence of Andreev levels is depicted depending on whether the system is in a singlet or doublet ground state (GS). Moreover, we demonstrate the variation of electrical conductance as a function of bias voltage $eV_{dc} = \mu_N - \mu_S$ for various values of on-dot Coulomb interaction U and Zeeman energy E_z in the non-linear regime.

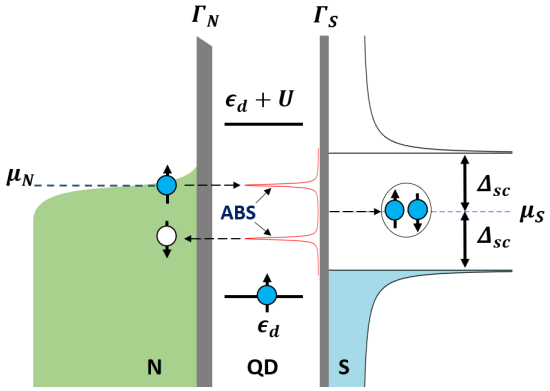

FIGURE 1. A schematic electronic band diagram of the hybrid N-QD-S system with tunnel couplings to normal metal and Superconductor Γ_N and Γ_S respectively. Δ_{sc} is the superconducting gap, and U is the Coulomb interaction or charging energy. The single-level QD with two effective levels at ε_d and $\varepsilon_d + U$ (due to finite U) is connected to normal and superconducting reservoirs with applied bias $\mu_N - \mu_S = eV_{dc}$ where μ_N and μ_S are the chemical potentials of the normal and superconducting reservoirs respectively.

MODEL HAMILTONIAN AND THEORETICAL FORMULATION

The Hamiltonian for the N-QD-S system where QD has a single level is modeled by a single impurity Anderson model (SIAM) and BCS Hamiltonian. The assumption of QD with a single level is reasonable if QD level spacing $\delta\varepsilon$ is larger than all other relevant energy scales. The Hamiltonian for the given system in second quantized notation is written as:

$$\hat{H} = \hat{H}_S + \hat{H}_{QD} + \hat{H}_N + \hat{H}_{S-QD} + \hat{H}_{N-QD} \tag{1}$$

where

$$\hat{H}_S = \sum_{kS,\sigma} \xi_{kS} c^\dagger_{kS,\sigma} c_{kS,\sigma} - \sum_{kS} (\Delta_{sc} c^\dagger_{kS,\uparrow} c^\dagger_{-kS,\downarrow} + h.c) \tag{2}$$

$$\hat{H}_{QD} = \sum_{\sigma} \varepsilon_{d\sigma} n_{d\sigma} + U n_{d\uparrow} n_{d\downarrow} \tag{3}$$

$$\hat{H}_N = \sum_{kN,\sigma} (\xi_{kN} c^\dagger_{kN,\sigma} c_{kN,\sigma} + h.c) \tag{4}$$

$$\hat{H}_{S-QD} = \sum_{kS,\sigma} (V_{kS} d^\dagger_\sigma c_{kS,\sigma} + h.c) \tag{5}$$

$$\hat{H}_{N-QD} = \sum_{kN,\sigma} (V_{kN} d^\dagger_\sigma c_{kN,\sigma} + h.c) \tag{6}$$

In equation (2), $\hat{H}_S$ is the BCS Hamiltonian, $c^\dagger_{kS,\sigma}$ ($c_{kS,\sigma}$) creates (destroys) an electron with spin $\sigma = \uparrow, \downarrow$ and wavevector k in the single-particle energy state ξ_{kS} of the superconducting lead. The first term in Eq. (2) describes the kinetic energy of the electrons while the second term represents the creation of the Cooper pair (two electrons with opposite momenta and spin) and the subsequent destruction of another Cooper pair. Δ_{sc} is the superconducting energy gap and describes the energy required to break a Cooper pair. The single electron energy $\xi_{kS} = \varepsilon_{kS} - \mu_S$ is referred with respect to the chemical potential at the superconducting reservoir $\mu_S = \varepsilon_f = 0$ at T = 0 K.

In equation (3), $\hat{H}_{QD}$ is the Hamiltonian for single level Quantum Dot, $d^\dagger_\sigma (d_\sigma)$ creates (destroys) an electron with spin $\sigma = \uparrow, \downarrow$ on the dot level with energy $\varepsilon_{d\sigma}$ and $n_{d\sigma} = d^\dagger_\sigma d_\sigma$ is the number operator. In the presence of an external magnetic field B, spin-degeneracy is broken and the quantum dot energy levels are given by, $\varepsilon_{d\sigma} = \varepsilon_d - \frac{\sigma E_z}{2}$ with $E_z = g\mu_B B$ being the Zeeman splitting energy. The second term in Eq.(3) describes the local on-dot Coulomb interaction U between electrons on the QD, which hinders getting an exact solution to the problem.

In equation (4), $\hat{H}_N$ describes the Hamiltonian for the normal reservoir with ξ_{kN} as the K.E of a free electron. In equations (5) and (6), $\hat{H}_{S-QD}$, $\hat{H}_{N-QD}$ describe the coupling between the QD level to the external superconducting and the normal lead respectively. V_{kS}, V_{kN} are the respective hybridization energies.

To diagonalize the BCS Superconducting part of the Hamiltonian in equation (1), we apply the unitary Bogoliubov transformation. After Bogoliubov transformation, the effective model Hamiltonian becomes,

$$\begin{aligned} \hat{H} = &\sum_{kS,\sigma} E_{kS} b^\dagger_{kS,\sigma} b_{kS,\sigma} + \sum_{\sigma} \varepsilon_d n_{d\sigma} + U n_{d\uparrow} n_{d\downarrow} + \sum_{kN,\sigma} (\xi_{kN} c^\dagger_{kN,\sigma} c_{kN,\sigma} + h.c) \\ &+ \sum_{k\sigma} (V_{kS} u^*_k d^\dagger_\sigma b_{k\sigma} + h.c) + \sum_{k} [V_{kS} v_k (d^\dagger_\uparrow b^\dagger_{-K\downarrow} - d^\dagger_\downarrow b^\dagger_{K\uparrow}) + h.c] + \sum_{kN,\sigma} (V_{kN} d^\dagger_\sigma c_{kN,\sigma} + h.c) \end{aligned} \tag{7}$$

Now, we can solve the above effective Hamiltonian by using Green's function equation of motion technique. As we are mainly interested in spectral and transport properties of the quantum impurity, it can be extracted from the single-particle retarded Green's function in Zubarev notation defined as,

$$G^r_{d\sigma}(t) = \langle\langle d_\sigma(t); d^\dagger_\sigma(0)\rangle\rangle = -i\theta(t)\langle[d_\sigma(t), d^\dagger_\sigma(0)]_+\rangle \tag{8}$$

Where $\theta(t)$ is the unit step or Heaviside step function. Now, the Fourier transform of the above retarded Green's function should satisfy the following equation of motion (EOM)

$$\omega\langle\langle d_\sigma; d^\dagger_\sigma\rangle\rangle_\omega = \langle[d_\sigma, d^\dagger_\sigma]_+\rangle + \langle\langle[d_\sigma, H]; d^\dagger_\sigma\rangle\rangle_\omega \tag{9}$$

In the presence of finite on-dot Coulomb interaction U, it hinders an exact solution to the problem which means the Hamiltonian is not exactly solvable due to the quartic term in the Coulomb interaction. This leads to a hierarchy of Green's function equation of motion that one needs to truncate by invoking some physical arguments i.e. Hartree-Fock (HF) mean-field approximation or some other higher-order decoupling schemes to obtain a closed set of coupled Green's function equations. Within the simple mean-field HF approximation, higher-order correlation functions are expressed as,

$$U\left\langle\left\langle\left[d_\uparrow, n_\uparrow n_\downarrow\right]|d^\dagger_\uparrow\right\rangle\right\rangle = U\left\langle\left\langle d_\uparrow n_\downarrow|d^\dagger_\uparrow\right\rangle\right\rangle = U\left\langle\left\langle d_\uparrow d^\dagger_\downarrow d_\downarrow|d^\dagger_\uparrow\right\rangle\right\rangle = U\langle n_\downarrow\rangle\left\langle\left\langle d_\uparrow|d^\dagger_\uparrow\right\rangle\right\rangle - U\langle d_\uparrow d_\downarrow\rangle\left\langle\left\langle d^\dagger_\downarrow|d^\dagger_\uparrow\right\rangle\right\rangle \tag{10}$$

In Nambu representation, the retarded Green's function of the quantum dot (QD) can be represented by 2×2 matrices:

$$G^r_d(\omega) = \left\langle\left\langle\begin{pmatrix} d_\uparrow \\ d^\dagger_\downarrow\end{pmatrix}\begin{pmatrix} d^\dagger_\uparrow & d_\downarrow\end{pmatrix}\right\rangle\right\rangle_\omega = \begin{pmatrix} \langle\langle d_\uparrow|d^\dagger_\uparrow\rangle\rangle_\omega & \langle\langle d_\uparrow|d_\downarrow\rangle\rangle_\omega \\ \langle\langle d^\dagger_\downarrow|d^\dagger_\uparrow\rangle\rangle_\omega & \langle\langle d^\dagger_\downarrow|d_\downarrow\rangle\rangle_\omega\end{pmatrix} = \begin{pmatrix} G^r_{d,11}(\omega) & G^r_{d,12}(\omega) \\ G^r_{d,21}(\omega) & G^r_{d,22}(\omega)\end{pmatrix} \tag{11}$$

By using Green's function EOM technique (Eq. 9), we obtain the close set of coupled equations, and after solving those set of coupled equations, the expression for the single electron retarded Green's function ($\langle\langle d_\sigma; d^\dagger_\sigma\rangle\rangle$) of the QD can be written as,

$$G^r_{d,11}(\omega) = \langle\langle d_\uparrow|d^\dagger_\uparrow\rangle\rangle_\omega = \frac{\omega + \varepsilon_{d\sigma-} + U\langle n_{d\sigma}\rangle + i\Gamma_N - I_1}{(\omega + \varepsilon_{d\sigma-} + U\langle n_{d\sigma}\rangle + i\Gamma_N - I_1)(\omega - \varepsilon_{d\sigma} - U\langle n_{d\sigma-}\rangle + i\Gamma_N - I_2) - (I_3 + U\langle d_\uparrow d_\downarrow\rangle)^2} \tag{12}$$

where I_1, I_2 are diagonal, and I_3 is the off-diagonal part of self-energy, which corresponds to the induced pairing due to the coupling between the quantum dot and superconducting lead. The expressions for I_1, I_2 and I_3 are

$$I_1 = I_2 = -\left[\frac{\Gamma_S\omega}{\sqrt{\Delta^2_{sc} - \omega^2}}\theta(\Delta_{sc} - |\omega|) + \frac{i|\Gamma_S|\omega}{\sqrt{\omega^2 - \Delta^2_{sc}}}\theta(|\omega| - \Delta_{sc})\right] \tag{13}$$

$$I_3 = -\left[\frac{\Gamma_S\Delta_{sc}}{\sqrt{\Delta^2_{sc} - \omega^2}}\theta(\Delta_{sc} - |\omega|) + \frac{i|\Gamma_S|\Delta_{sc}}{\sqrt{\omega^2 - \Delta^2_{sc}}}\theta(|\omega| - \Delta_{sc})\right] \tag{14}$$

where the coupling to the superconducting and the normal lead in wide-flat band limit is given by $\Gamma_S = \pi\rho_{0S}|V^2_{kS}|$, $\Gamma_N = \pi\rho_{0N}|V^2_{kN}|$ respectively and $\rho_{0\alpha}$ is the density of states at the Fermi energy of contact α (= S, N) in the normal phase. The explicit form of $G^{r,HF}_d(\omega)$ becomes

$$G^{r,HF}_d(\omega) = \frac{1}{D(\omega)}\begin{pmatrix} \omega + \varepsilon_{d\sigma-} + U\langle n_{d\sigma}\rangle + i\Gamma_N + \frac{\Gamma_S\omega}{\sqrt{\Delta^2_{sc}-\omega^2}} & \frac{\Gamma_S\Delta_{sc}}{\sqrt{\Delta^2_{sc}-\omega^2}} + U\langle d_\uparrow d_\downarrow\rangle \\ \frac{\Gamma_S\Delta_{sc}}{\sqrt{\Delta^2_{sc}-\omega^2}} + U\langle d^+_\downarrow d^+_\uparrow\rangle & \omega - \varepsilon_{d\sigma} - U\langle n_{d\sigma-}\rangle + i\Gamma_N + \frac{\Gamma_S\omega}{\sqrt{\Delta^2_{sc}-\omega^2}}\end{pmatrix} \tag{15}$$

We are interested in solving $\hat{H}$ to obtain the energy spectrum. For that purpose, we obtain the poles of the Green's function (i.e. equating denominator equal to zero) as, $D(\omega) \equiv Det[G^{r,HF}_d(\omega)^{-1}] = 0$ gives the Andreev-level spectrum of the system. The average occupation number $\langle n_{d\sigma}\rangle = -\frac{1}{\pi}\int_{-\infty}^{\infty} Im\langle\langle d_\sigma|d^\dagger_\sigma\rangle\rangle d\omega$ at the QD level of a given spin and the pairing parameter $\langle d_\uparrow d_\downarrow\rangle = \langle d^\dagger_\downarrow d^\dagger_\uparrow\rangle = -\frac{1}{\pi}\int_{-\infty}^{\infty} Im\langle\langle d^\dagger_\downarrow|d^\dagger_\uparrow\rangle\rangle d\omega$ have to be calculated self-consistently. The spectral function gives the energy resolution for a given quantum state. It indicates the distribution of excitations when a particle with certain quantum numbers is added to a given system. Thus, the QD spectral function is defined as, $\rho_d(\omega) = -\frac{1}{\pi}ImTr[G^{r,HF}_d(\omega)]$.

Such subgap spectrum can be obtained experimentally by measuring the differential conductance $G = \frac{dI}{dV_{dc}}$ where I is the electrical current when a DC bias voltage (V_{dc}), $eV_{dc} = \mu_N - \mu_S$ is applied between the contacts. Here, we set $\mu_S = 0$, only changing the chemical potential of the normal metal; thus, the applied bias voltage is $V_{dc} = \mu_N$. In

this non-linear regime, the total current can be decomposed into Andreev (A) and quasi-particle current (QP) currents, $I = I_A + I_{QP}$. For voltages $eV_{dc} \leq \Delta_{sc}$, the quasi-particle current is zero, $I_{QP} = 0$, and the only contribution comes from Andreev processes. For the opposite voltage limit, the quasi-particle current contribution is also finite and they can be expressed in the Landauer-type form [15]

$$I_A(V) = \frac{2e}{h}\int d\omega T_A(\omega)[f(\omega - eV_{dc}) - f(\omega + eV_{dc})] \tag{16}$$

$$I_{QP}(V) = \frac{2e}{h}\int d\omega T_{QP}(\omega)[f(\omega - eV_{dc}) - f(\omega)] \tag{17}$$

with the Fermi-Dirac distribution $f(\omega) = [\exp(\frac{\omega}{K_B T}) + 1]^{-1}$. Here, e and h denote the magnitude of the electronic charge and Planck's constant, respectively and the prefactor 2 is due to the spin degeneracy. The Andreev and quasi-particle transmission are defined as,

$$T_A(\omega) = \Gamma_N^2 |G^r_{d,12}(\omega)|^2 \tag{18}$$

$$T_{QP}(\omega) = \frac{\Gamma_N \Gamma_S |\omega|}{\sqrt{\omega^2 - \Delta_{sc}^2}}\theta(|\omega| - \Delta_{sc}) \times \left[|G^r_{d,11}(\omega)|^2 + |G^r_{d,12}(\omega)|^2 - \frac{2\Delta_{sc}}{|\omega|} Re(G^r_{d,11}(\omega)[G^r_{d,12}(\omega)]^*)\right] \tag{19}$$

In the next section, we will discuss the results obtained by the numerical computations for various parameter regimes.

RESULTS AND DISCUSSION

In this section, we present the numerical results obtained using MATLAB coding language. Our primary aim is to study the effect of U and the external magnetic field on the Andreev Bound states (ABSs) energy and non-linear electrical Conductance.

Let us start by considering an uncorrelated QD, which is equivalent to a spinless impurity. In Figure 2(a), energies of the sub-gap ABSs are plotted as a function of superconducting gap Δ_{sc}. The strong coupling Γ_N to the normal lead can increase the sub-gap state broadening (i.e., the reduction of the lifetime of quasiparticles) [11]. We can notice that Andreev bound states appear near the gap edge singularities $\pm\Delta_{sc}$ (when $\Delta_{sc} \ll \Gamma_S$) [16], and they evolve into subgap peaks (when $\Delta_{sc} \gg \Gamma_S$). Figure 2(b) & 2(c) presents the spectral density $\rho_d(\omega)$ as a function of the energy gap for ε_d = 0 and - Γ_S respectively and similar nature of ABSs spectrum appears here as in figure 2(a). In both cases, the sub-gap Andreev bound states gradually emerge from the gap edge singularities $\pm\Delta_{sc}$ (when $\Delta_{sc} \ll \Gamma_S$), and they evolve to well-defined subgap quasiparticle peaks (when $\Delta_{sc} \gg \Gamma_S$). When $\Delta_{sc} \ll \Gamma_S$, sub-gap quasiparticle peaks marges to each other and becomes a single broad peak as in the case of normal metal, centered at $\varepsilon_d = 0$ [figure 2(b)], while for figure 2(c), it shifts at $\varepsilon_d = -\Gamma_S$.

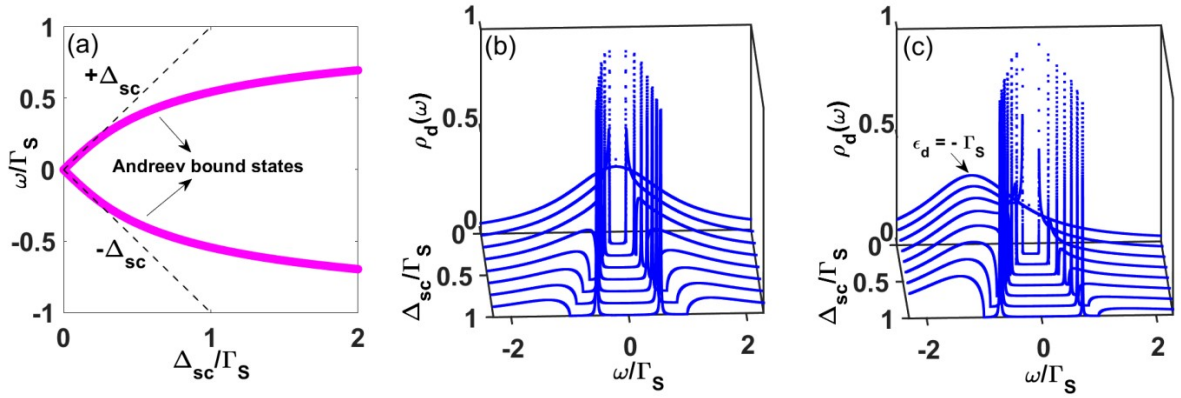

FIGURE 2. (a) The energies of the sub-gap Andreev bound states as a function of Δ_{sc}/Γ_S for an uncorrelated quantum dot ($\varepsilon_d = 0$) with weak coupling to the metallic lead i.e. $\Gamma_N = 0.001\Gamma_S$. The dashed lines indicate the gap edges $\pm\Delta_{sc}$, Figure (b) & (c) shows the spectral density $\rho_d(\omega)$ of an uncorrelated quantum dot obtained for the case when ε_d = 0 (left panel) and ε_d = - Γ_S (right panel) weakly coupled to the metallic lead, $\Gamma_N = 0.001\Gamma_S$.

In figure 3, we show the Andreev bound states of an uncorrelated quantum dot with respect to the dot energy ε_d for zero Zeeman splitting and compare this to the case of finite Zeeman splitting. We can observe that the number of bound states is double in the case of finite Zeeman splitting as the spin-up and spin-down level contribution is different while this contribution is equal for zero Zeeman field due to the degeneracy of spin-up and spin-down level (i.e., spin-independent).

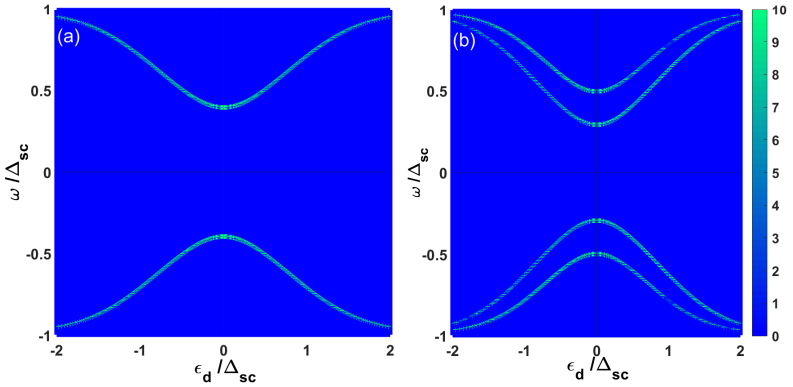

FIGURE 3. (a) Andreev bound states (ABSs) of an uncorrelated quantum dot as a function of quantum dot energy level $\varepsilon_d/\Delta_{sc}$ in the absence of external Zeeman field. (b) ABSs vs. dot energy level for finite Zeeman field.

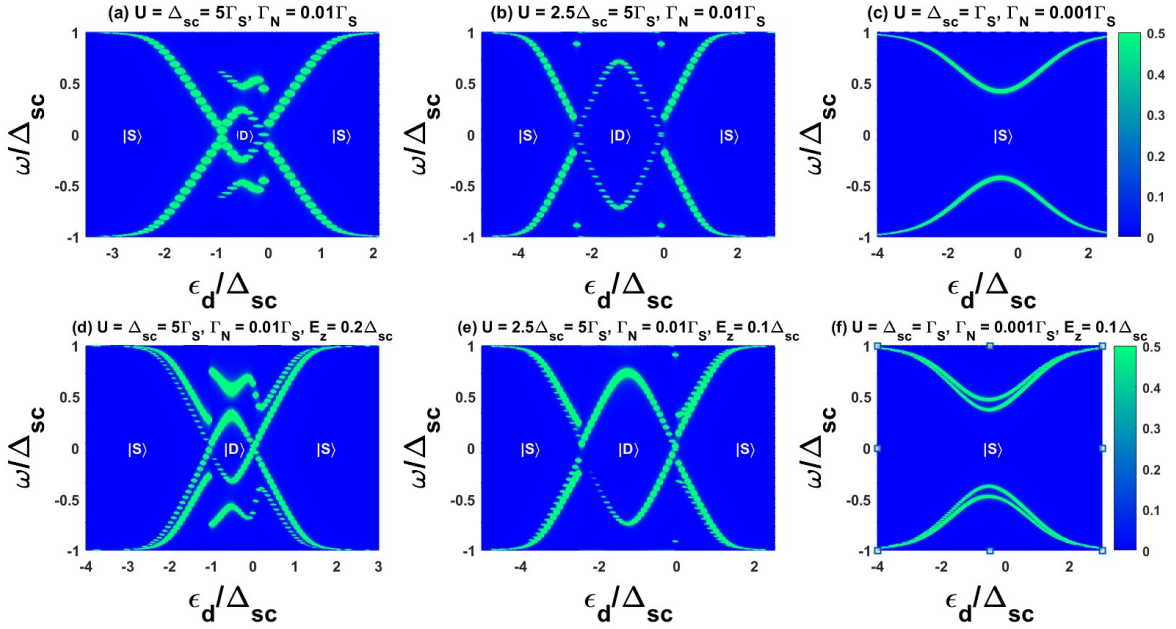

FIGURE 4. Top row depicts subgap ABSs as a function of quantum dot energy level $\varepsilon_d/\Delta_{sc}$ and coulomb interaction U/Δ_{sc} in the absence of external Zeeman field whereas the bottom row describe the effect of an external magnetic field B on the sub-gap Andreev levels. (These are the colormap plots where the colorbar represents the spectral density $\rho_d(\omega)$ in which the blue color corresponds to $\rho_d(\omega) = 0$ and the green color corresponds to $\rho_d(\omega) = 1$ respectively.)

Now, let us discuss the nature of ABSs as a function of quantum dot energy level $\varepsilon_d/\Delta_{sc}$ with finite on-dot Coulomb interaction U/Δ_{sc} in the absence as well as in the presence of external Zeeman field [figure 4] [12, 13]. For interacting QD, the average occupation number $\langle n_{d\sigma}\rangle$ at the QD level of a given spin σ and the pairing parameter $\langle d_\uparrow d_\downarrow\rangle$ are calculated self consistently and results in a singlet–doublet crossover occurring at larger values of U [13]. Let us first consider the left-most plot from the top row of Figure 4, and we found that ABSs form a loop structure between the two crossings that represents the quantum phase transition from a singlet to a doublet GS as reported experimentally in [12] for the Kondo regime. Also, we show that the sub-gap Andreev bound state exhibits anticrossing around the degenerate mean-field point $\varepsilon_d = -U$ and $\varepsilon_d = 0$. Now we are able to conclude that on the left ($\varepsilon_d < -U$) and right ($\varepsilon_d > 0$) sides of the plot, QD lies deep inside the singlet GS regime. But, as long as we move toward the central region ($-U \leq \varepsilon_d \leq 0$), the two subgap resonances approach each other and cross at the singlet–doublet phase boundaries, resulting in a quantum phase transition from a singlet GS to a doublet ground state. The quantum phase transition and the nature of ABSs depend on the ratio U/Δ_{sc}, $\varepsilon_d/\Delta_{sc}$, Δ_{sc}/Γ_S. At the singlet-doublet transition, the upper and lower ABSs cross each other. In the singlet region, only two ABSs appear symmetrically with respect to the Fermi level, whereas in the doublet case, the number of ABS is doubled [see first and second columns in Figure 4]. As Γ_S is increased, our result displays the disappearance of loop structure [see the third column in Figure 4]. The appearance of the outer ABS is an artifact of HF approximation and has not been observed experimentally. These outer ABS merges with the quasiparticle states for increasing U. Next, the bottom row refers to the effect of B on the Andreev levels, which results in two distinct excitations in the case of singlet ground state (GS) where the Zeeman effect splits the spin degeneracy of doublet excited state (ES). In contrast, there will not be any splitting in the case of doublet GS, as the state has an odd number of electrons present. These results are in good qualitative agreement with the experimental

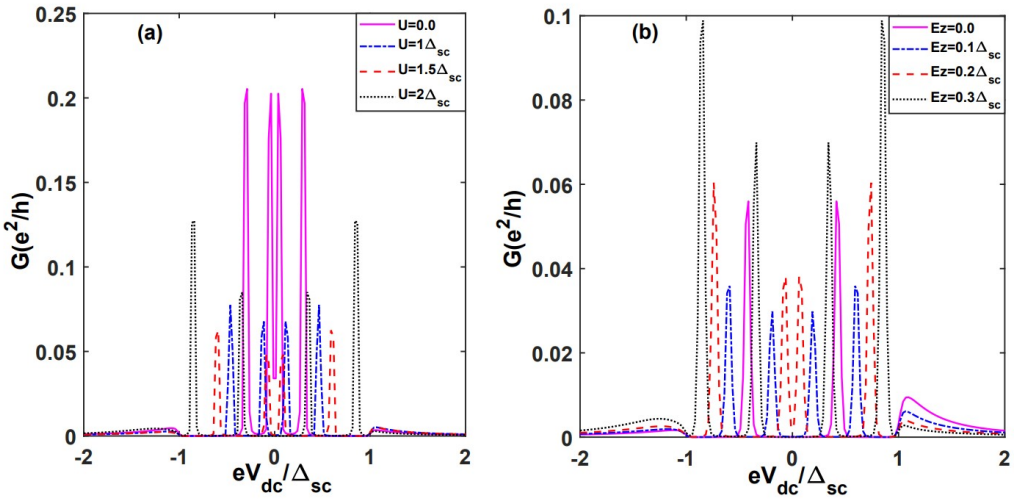

FIGURE 5. Non-linear electrical conductance G as a function of bias voltage V_{dc} for (a) several values of on-site Coulomb interaction U with finite Zeeman energy $E_z = 0.3\Delta_{sc}$, $\Gamma_N = 0.01\Delta_{sc}$, $\Gamma_S = 0.2\Delta_{sc}$ and $K_BT = 0.001\Delta_{sc}$ at $\varepsilon_d = -U/2$. (b) different values of Zeeman energy E_z at fixed value of on-site Coulomb interaction U = $2\Delta_{sc}$. The other parameters are $\Gamma_N = 0.01\Gamma_S$, $\Gamma_S = 0.2\Delta_{sc}$ and $K_BT = 0.01\Delta_{sc}$.

results [12].

We also consider the case when the system is under the influence of voltage biasing. Figure 5 shows the non-linear conductance dI/dV_{dc} as a function of biased voltage for (a) different values of on-dot Coulomb interactions U values and (b) different values of Zeeman energy E_z. For relatively low temperatures, the competition between Andreev tunneling and finite Coulomb interaction may lead to additional splitting of the U = 0 subgap Andreev peaks and develops a local minimum close to zero biasing, which is absent in the case of an uncorrelated quantum dot (QD). Now, the application of a magnetic field generates additional splitting of subgap Andreev peaks even for an uncorrelated case, and sharp peaks are observed for the finite Coulomb interaction case with a local minimum close to zero biasing. Also, Figure 5(b) shows the additional splitting of subgap peaks due to the influence of various values of the Zeeman field, though it is found that there is no splitting of ABS for zero splitting energy.

CONCLUSION

In summary, the Bogoliubov transformation, followed by the Hartree-Fock (HF) mean-field approach, is employed to understand the nature of sub-gap ABSs in the presence of the external Zeeman field at the N-QD-S system in the Coulomb blockade regime. At first, we start with an uncorrelated quantum dot and analyze the nature of ABSs at two different quantum dot energy levels. After that, when it is exposed to the external magnetic field, it is observed that the finite Zeeman field can split the subgap levels into two due to different spin level contributions. Next, we move to the case of correlated (interacting) quantum dot, where we analyze the QD's spectral density to study the ABSs as a function of dot parameters and we show singlet to doublet transition in the absence of a magnetic field and splitting of ABSs in the singlet GS due to finite Zeeman field. A similar observation can be found in the case of electrical conductance as a function of bias voltage for various values of on-site Coulomb interaction and Zeeman energy. In this study, we have analyzed the spectral and transport properties of the weakly correlated N-QD-S system in the presence of an external magnetic field, and this work can be extended to the strongly correlated region and to address more properties like electrical, thermoelectric, etc.

ACKNOWLEDGMENTS

We would like to acknowledge the Ministry of Human Resource Development (MHRD), India, for their financial support in the form of a Ph.D. fellowship.

REFERENCES

1. M. A. Kastner, "Artificial Atoms," Physics Today, 46, 1, 24–31, 1993.
2. E. Liebhaber et al., "Quantum spins and hybridization in artificially-constructed chains of magnetic adatoms on a superconductor," Nature Communications, 13, 1, 2022.
3. R. S. Deacon et al., "Tunneling Spectroscopy of Andreev Energy Levels in a Quantum Dot Coupled to a Superconductor," Physical Review Letters, 104, 7, 2010.
4. V. Mourik, K. Zuo, S. M. Frolov, S. R. Plissard, E. P. A. M. Bakkers, and L. P. Kouwenhoven, "Signatures of Majorana Fermions in Hybrid Superconductor-Semiconductor Nanowire Devices," Science, 336, 6084, 1003–1007, 2012.

5. J.-D. Pillet, C. H. L. Quay, P. Morfin, C. Bena, A. L. Yeyati, and P. Joyez, "Andreev bound states in supercurrent-carrying carbon nanotubes revealed," Nature Physics, 6, 12, 965–969, 2010.
6. T. Dirks et al., "Transport through Andreev bound states in a graphene quantum dot," Nature Physics, 7, 5, 386–390, 2011.
7. R. C. Jaklevic, J. Lambe, A. H. Silver, and J. E. Mercereau, "Quantum Interference Effects in Josephson Tunneling," Physical Review Letters, 12, 7, 159–160, 1964.
8. W.-J. Gong, Y.-L. Zhu, X.-Q. Wang, and H.-N. Wu, "Enhancement of the Cooper-pair splitting in the Fano interferometer," EPL (Europhysics Letters), 114, 4, 47010, 2016.
9. J. Clarke and F. K. Wilhelm, "Superconducting quantum bits," Nature, 453, 7198, 1031–1042, 2008.
10. J. Kong et al., "Quantum Interference and Ballistic Transmission in Nanotube Electron Waveguides," Physical Review Letters, 87, 10, 2001.
11. J. Barański and T. Domański, "In-gap states of a quantum dot coupled between a normal and a superconducting lead," Journal of Physics: Condensed Matter, 25, 43, 435305, 2013.
12. E. J. H. Lee, X. Jiang, M. Houzet, R. Aguado, C. M. Lieber, and S. De Franceschi, "Spin-resolved Andreev levels and parity crossings in hybrid superconductor–semiconductor nanostructures," Nature Nanotechnology, 9, 1, 79–84, 2013.
13. S. Verma, "Influence of superconductivity on the magnetic moment of quantum impurity embedded in BCS superconductor," Journal of Physics: Condensed Matter, 33, 8, 085603, 2020.
14. J. S. Lim and R. López, "Subgap spectrum for an interacting hybrid superconducting quantum dot," Physical Review B, 101, 24, 2020.
15. M. Krawiec and K. I. Wysoki ski, "Electron transport through a strongly interacting quantum dot coupled to a normal metal and BCS superconductor," Superconductor Science and Technology, 17, 1, 103–112, 2003.
16. J. Bauer, A. Oguri, and A. C. Hewson, "Spectral properties of locally correlated electrons in a Bardeen–Cooper–Schrieffer superconductor," Journal of Physics: Condensed Matter, 19, 48, 486211, 2007.
17. M. Eto and Y. V. Nazarov, "Mean-field theory of the Kondo effect in quantum dots with an even number of electrons," Physical Review B, 64, 8, 2001.